Department of Electronics, Electricity and Computer Sciences
Transmission & Distribution of Electrical Energy

Power Line Aeolian Vibrations.

Prepared by:

Pr. J-L Lilien

November, 2013

Table of Contents

Table des matières

1 Introduction

Aeolian vibration is a low amplitude (conductor diameter) high frequency (5 to 150 Hz) phenomenon. Aeolian vibration is one of the most important problems in transmission lines because it represents the major cause of fatigue failure of conductor strands or of items associated with the support, use, and protection of the conductor. In this phenomenon, conductor strand fatigue failures occur at the suspension clamps or at the clamps of the other devices installed on the conductor such as spacers, spacer dampers, dampers and other devices.

Fig 2.1 typical broken strand due to aeolian vibration after removal of suspension clamp.

Forces induced by vortex shedding are the cause of this type of vibration (Blevins-1990, Buckner 1968, Claren et al 1969 & 1974).

The response of the conductor to vortex shedding excitation is strongly non linear in terms of the vibration amplitude. This non-linearity is related to both the conductor parameters and the characteristics of the wind blowing across the conductor.

In this phenomenon, maximum vibration amplitudes can be, at maximum, about one conductor diameter (peak-to-peak) where they can cause fatigue of the conductor strands due to bending. The problem may be defined as controlling the conductor vibration amplitude in order to maintain the stress in the conductor strands below the fatigue endurance limit. Adequate control can be achieved if the correct amount of damping is present in the system and if necessary, additional damping can be introduced in the form of damping devices such as dampers and spacer-dampers.

The complex phenomenon of vortex shedding (fig. 2.2), from an engineering point of view is simplified through an approach known as ‘Energy Balance Principle’ (EBP): this approach does not reproduce all the phenomenon features but allows for the definition of the maximum vibration amplitudes undergone by the conductor due to aeolian vibrations: the steady state amplitude of vibration of the conductor or bundle due to aeolian vibration is that for which the energy dissipated by the conductor and other devices used for its support and protection, equals the energy input from the wind.

The energy introduced by the wind to single and bundle conductors has been determined through wind tunnel measurements. Vortex shedding excitation on a vibrating cylinder, as already said, is quite a complicated phenomenon, which will cover aspects as vortex shedding frequency, lock-in, synchronization range, modes of vortex shedding, variables controlling the phenomenon and energy input for both single and bundle conductors. The energy dissipated by the conductor and damping devices can be determined through laboratory measurements

From the comparison between introduced and dissipated energies, the steady state amplitude of vibration (fig 2.3 and 2.4) of the conductor can be evaluated together with strains and stresses in its most significant sections.

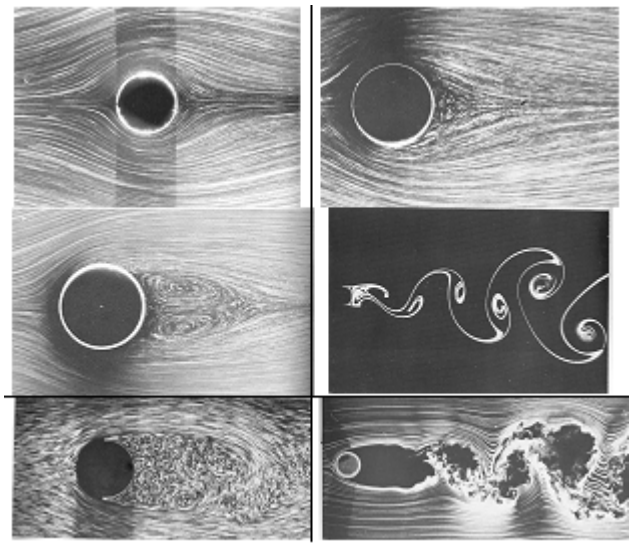

Fig 2.2 Flow visualization; identification according to (row, column): (1,1) *R*=1.1 (Taneda) , (1,2) *R*=9.6 (Taneda), (2,1) *R*=26 (Taneda), (2,2) *R*=140 (Taneda), (3,1) *R*=2000 (Werlé & Gallon), (3,2) *R*=10000 (Corke & Nagib)

Fig 2.3 Transient response measured at the antinode of an aero elastic model of a conductor after Brika & Laneville (1993)

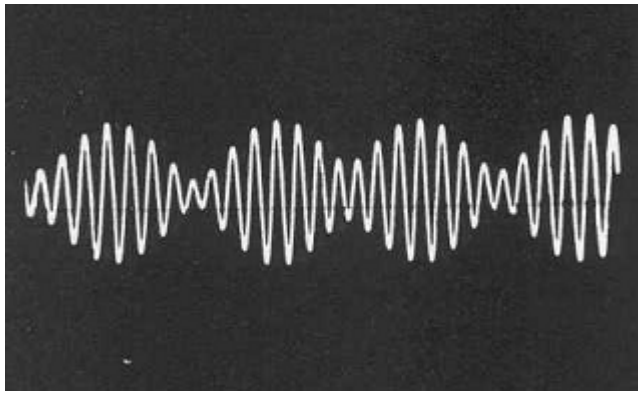

Fig 2.4 record of natural Aeolian vibrations (EPRI 1979). Amplitude vs time.

2 General Approach

Under moderate wind speed (generally lower than 7 m/s) Von Karman vortex shedding will induce vertical vibrations at frequencies depending on the Strouhal relationship (the Strouhal number is about 0.185 for all typical power lines cables) :

$$f = 0.185\frac{V}{D} \qquad \text{(eq 3.1)}$$

Where V is the wind speed (m/s), D the conductor diameter (m) and f the vibration frequency (Hz).
Thus a given diameter and a given wind speed are giving a frequency of vibration. That frequency is always close to an eigenfrequency of the span concerned as these frequencies are very close to each other, separated by the basic frequency, close to 0.1 to 0.5 Hz. It is generally a very high mode number (20 to 80 f.e.) which means numerous loops in one span (fig 3.1). The loop length is simply given by the ratio between the the wave propagation speed (= square root of the ratio tension/mass) and the frequency of vibration, generally the wave length is about some meters.

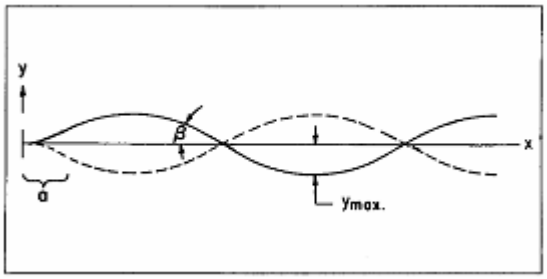

fig 3.1 typical wave shape during Aeolian vibration

Example : twin 2x620 mm2 AMS tensioned at 35000 N/conductor on a span length of 350m. The subconductor of 620 mm2 has 32.4 external diameter and a mass of 1.7 kg/m. Sag can be estimated at 7.3 m (ratio sag/span = 2.1%)
Wave propagation speed : sqrt (35000/1.7) = 143 m/s
Basic swing frequency : (0.56/sqrt(sag))= 0.21 Hz
The aeolian vibration frequencies are (range wind speed 0.5 to 7 m/s) : 3 Hz to 40 Hz
Wave length of these frequencies : 48 m (3 Hz) to 3.6 m (40 Hz).

The Energy Balance Principle (EBP) (wind power in = self dissipation + damper out) is used for analysis of the system, it helps to define amplitudes of vibrations at each frequencies.
Next steps are evaluating maximum bending strains in the conductor to evaluate its protection against Aeolian vibration and to highlight, if any, dangerous frequency ranges. Dangerous range are linked to fatigue limit of the corresponding cable+fixation system.

One hour vibrations at 20 Hz every day would means 26 Megacycles per year.

To apply EBP numerous investigations have been done to determine basic inputs to be used.

2.1 Conductor self damping

A stranded conductor will consume energy when it is bended, mainly due to friction between the strands as they moved relatively to each other. The dissipation energy increases with increasing frequency, amplitude and conductor diameter. (Electra-1979) Conductor self-dissipation, it is a function of static tensile stress in the Aluminium layers. The higher the tensile stress, the tighter the layers will lock, and the less inter-strand friction, which is the main source of self-dissipation, will take place when the conductor is curved during vibration.

Conductor self dissipation may be calculated by the empirical rules (*Electra 1988)*:

$$P_C = k\frac{A^l f^m}{T^n} \qquad \text{[W/m]} \qquad (eq\ 3.2)$$

where:

P_c	=	power per unit length dissipated in the conductor	[W/m]
k	=	factor of proportionality	[see below for unit]
A	=	Maximum Amplitude (pk-pk)	[m]
f	=	frequency	[Hz]
T	=	Conductor tension	[kN]

The conductor “k” factor is a special function involving the diameter, rated strength, and mass per unit length of a conductor [*EPRI 1979*].

$$k = \frac{d}{\sqrt{RS \times m}} \qquad (eq\ 3.3)$$

Where d is a conductor diameter [mm], RS is rated strength [kN], m is mass per unit length [kg/m].

Quantities *l, m* and *n* are amplitude exponent, frequency exponent and tension exponent respectively. These exponents are investigated by many investigators varies a quite a bit (see table 3.1, Electra 1988).

It is to be noted that moderate differences in the exponent values lead to huge differences in the self-damping values.

Table 3.1 : Exponent values for self-dissipation

Investigators	l	m	n	Method	Span Length, m
Tompkins	2.3 - 2.6	5.0 - 6.0	1.9	ISWR	36
Claren & Diana	**2**	**4**	**2.5; 3.0; 1.5**	**P.T**	**46**
Seppa	2.0-3.0	5.0-6.0	2.0-3.0	ISWR	36
Rawlins	2.2	5.4		ISWR	36
Lab.A	2	4		P.T	46
Lab.B	2.2	5.2		P.T	30
Lab.C	2.44	5.5		ISWR	36
Kraus & Hagedorn	2.47	5.38	2.8	P.T	30
Noiseux	**2.44**	**5.63**	**2.76**	**ISWR**	**63**
Tavano	1.9 -2.3	3.8 -4.2		P.T	92
Mocks & Schmidt	2.45	5.38	2.4	P.T	30

ISWR : Inverse Standing Wave Ratio Method
PT: Power Method

For example, Noiseux' s exponents may be used as follows to calculate the self-dissipation power (Pc) of conductor :

$$P_C = k \frac{A^{2.44} f^{5.63}}{T^{2.76}} \qquad \text{[W/m]} \qquad (eq\ 3.4)$$

For reduced self-dissipation the formula shall be;

$$\frac{P_C}{f^3 d^4} = k \frac{1}{d^{1.56} T^{2.76}} f^{2.63} \left[\frac{A}{d}\right]^{2.44} \qquad \text{[W. s}^3\text{/m}^5\text{]} \qquad (eq\ 3.5)$$

There exist IEEE recommendations to perform appropriate testsing to evaluate Pc with a good level of precision on a test bench (IEEE- 1993 and Electra-1979).

Visualisation of reduced self dissipation is shown on fig 3.2 and 3.3 with different scaling.

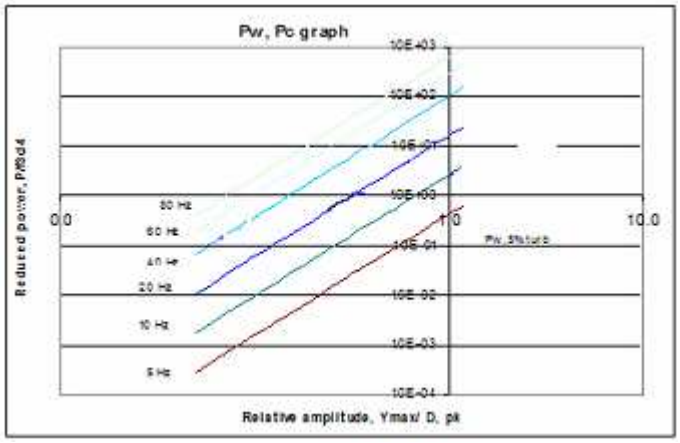

Fig 3.2 Reduced power dissipation, an example (log scale)

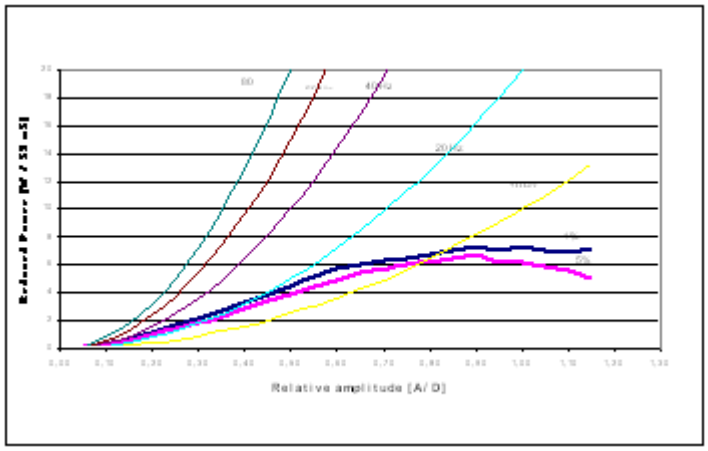

Figure 3.3 Results of Power dissipation (Bear conductor at 20% UTS) (linear scales). The two extra curves are the wind power input (see later).

It must be noted that there are big discrepancies between actual value and formula as detailed in (Electra – 1988) and shown on fig 3.4.

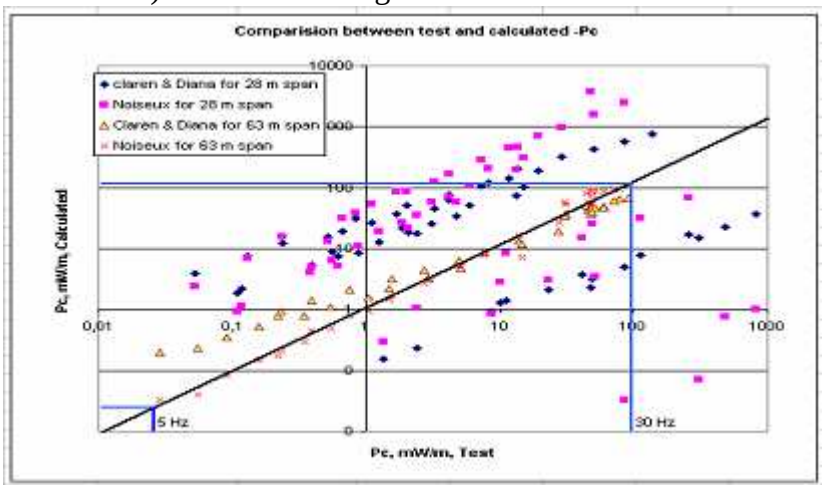

Figure 3.4 : Data scattering of Conductor self dissipation. Dots are covering all ranges of frequencies and amplitudes.

More recently, a better model has been developed based on a needed test lab on a conductor sample. That test is purely a static test and is evaluating a hysteresis curve representative of the inter-strand friction. More is detailed in the exercise proposed to the student.

2.2 Wind power input

The mechanical power transferred from the wind to a vibrating conductor may be expressed in the general form:

$$P_W = Lf^3D^4F\left(\frac{A}{D}\right) \qquad \text{(eq 3.6)}$$

Where P_W = mechanical power imparted by the wind to the whole span of a conductor (W)

A = vibration amplitude (m)

L = span length (m)

f = frequency of vibration in (Hz)

D = diameter of conductor in (m)

$F\left(\frac{A}{D}\right)$ = a function of the vibration amplitude

$F\left(\frac{A}{D}\right)$ is a nonlinear function of the dimensionless vibration amplitude. Several laboratories have tried to express the $F\left(\frac{A}{D}\right)$. Their results however differ a lot even shown in logarithmic scale. This is because the measurements of these small energy levels (fractions of a watt per meter of conductor) are very sensitive to disturbances. $F\left(\frac{A}{D}\right)$ is given in [Rawlins- 1998] for different turbulence levels (1, 5, 10, 15, 20%)
An example of wind power curves for different turbulence levels is given in fig. 3.5.

Alcoa Laboratories has made a study in terms of parameter, related to a wind power input, which is a function of reduced velocity Vr, dimensionless amplitude [Y/d], and reduced decrement δ_r .The reduced decrement can be converted in reduced wind power, $P_W \big/ f^3 d^4$, through this relationship.

$$\frac{P_W}{f^3 d^4} = \rho\delta_r \frac{\pi^2}{4}\left[\frac{Y_{\max}}{d}\right]^2 \qquad [\text{W.s}^3/\text{m}^5] \qquad \text{(eq 3.7)}$$

Where ρ = mass density of the fluid medium; 1.2 kg/m3

δ_r = reduced decrement

The value of reduced decrement, δ_r , for different amplitude and for different level of turbulence studied by Alcoa Laboratories are given table 3.2 below ***(Rawlins- 1998)***

The reduced wind power, $\frac{P_w}{f^3 d^4}$, which is a function of relative amplitude, has been drawn for different level of turbulence, see *figure 3.5*. Increasing the turbulence level decreases the wind power input.

Turbule	1%	5%	10%	15%	20%		Turb	1%	5%	10%	15%	20%
Ymax/D		δ_y					Ymax/D		Pw / f3 d4			
0,05	19,3	12,6	9,1	7,09	5,77		0,05	0,15	0,09	0,07	0,05	0,04
0,10	11,9	9,6	6,9	5,31	4,22		0,10	0,35	0,28	0,21	0,16	0,12
0,15	10,6	8,6	6,2	4,66	3,61		0,15	0,71	0,57	0,41	0,31	0,24
0,20	9,8	8,1	5,9	4,46	3,45		0,20	1,16	0,96	0,70	0,53	0,41
0,25	9,0	7,5	5,6	4,23	3,26		0,25	1,66	1,38	1,04	0,78	0,60
0,30	8,2	7,0	5,4	4,10	3,18		0,30	2,19	1,87	1,44	1,09	0,85
0,35	7,4	6,4	5,0	3,77	2,87		0,35	2,67	2,30	1,81	1,37	1,04
0,40	6,8	6,0	4,8	3,65	2,78		0,40	3,24	2,86	2,29	1,73	1,32
0,45	6,5	5,7	4,6	3,53	2,68		0,45	3,89	3,39	2,77	2,12	1,61
0,50	6,0	5,3	4,4	3,38	2,57		0,50	4,47	3,92	3,26	2,50	1,90
0,55	5,8	5,0	4,1	3,17	2,41		0,55	5,20	4,44	3,71	2,84	2,16
0,60	5,3	4,6	3,8	2,90	2,15		0,60	5,69	4,85	4,05	3,09	2,29
0,65	4,8	4,3	3,6	2,72	1,99		0,65	6,03	5,40	4,50	3,40	2,49
0,70	4,4	3,9	3,3	2,50	1,83		0,70	6,34	5,63	4,76	3,63	2,66
0,75	3,9	3,6	3,1	2,32	1,67		0,75	6,48	6,03	5,13	3,86	2,78
0,80	3,6	3,2	2,8	2,13	1,53		0,80	6,77	6,14	5,31	4,04	2,90
0,85	3,3	3,0	2,6	2,01	1,44		0,85	7,06	6,48	5,65	4,30	3,08
0,90	3,0	2,8	2,4	1,84	1,31		0,90	7,10	6,67	5,80	4,41	3,14
0,95	2,6	2,3	2,1	1,56	1,09		0,95	7,00	6,15	5,48	4,17	2,91
1,00	2,4	2,1	1,9	1,40	0,95		1,00	7,19	6,13	5,51	4,15	2,81
1,05	2,2	1,8	1,6	1,21	0,81		1,05	7,05	5,81	5,26	3,95	2,64
1,10	1,9	1,6	1,4	1,01	0,63		1,10	6,81	5,62	5,02	3,62	2,26
1,15	1,8	1,3	1,2	0,84	0,52		1,15	7,17	4,93	4,50	3,29	2,04
1,20	2,1	1,0	1,0	0,74	0,47		1,20	8,87	4,39	4,14	3,16	2,00

Table 3.2 **: Reduced decrement and reduced wind power**

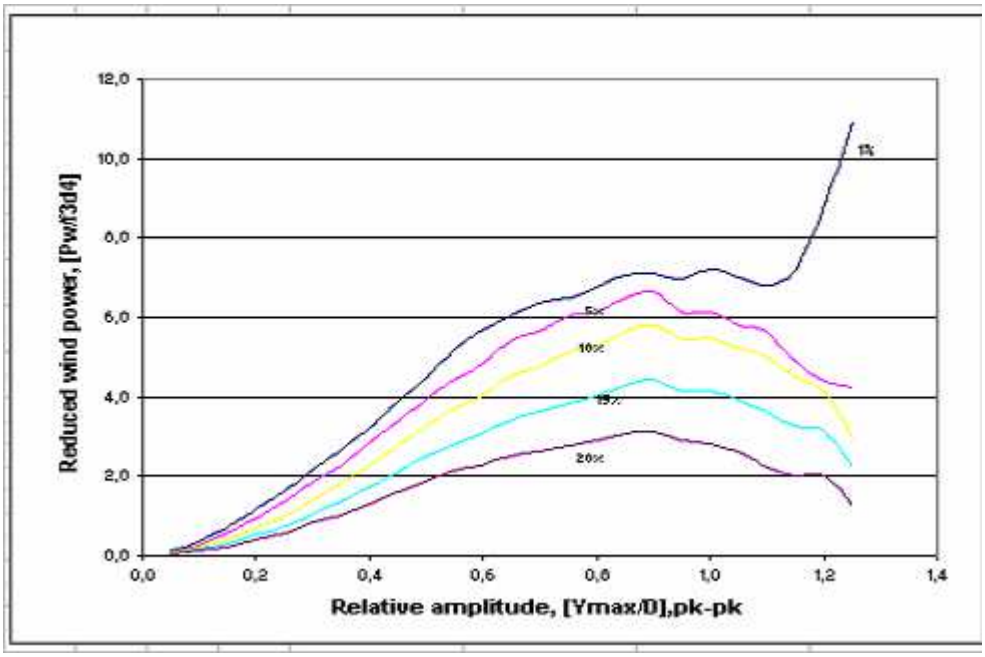

Figure 3.5 : Reduced Wind power for different level of turbulence

3 Energy Balance Principle

In a wind, with a defined turbulence (1% to 20%), the vibration level can be estimated by using the Energy Balance Principle (EBP). This is based on presumed knowledge of (Hagedorn 1982 , Electra-1988, Verma 2003, Electra-2005 b):

- Energy imparted to the conductor by the wind (fig 3.5 and table 3.2)
- Energy dissipated by the transmission line conductor (formula 3.2 and table 3.1)
- Energy dissipated by the dampers. (see later)

As a vibrating conductor with fittings receives energy from the wind, its amplitude will obviously rise to a point at which its internal dissipation balances the energy input from the wind. This is expressed in the following equation of the EBP:

$$P_W = P_C + P_D . \qquad \text{(eq 4.1)}$$

Here, P_W is the power imparted by the wind; P_C the power dissipated by the self-damping of the conductor, and P_D the power dissipated by the damper. Each of these terms is a function of the frequency and amplitude of the conductor oscillations. For a given wind speed, or frequency, the equation (eq 4.1) is a nonlinear algebraic equation in the amplitude of conductor oscillations only.

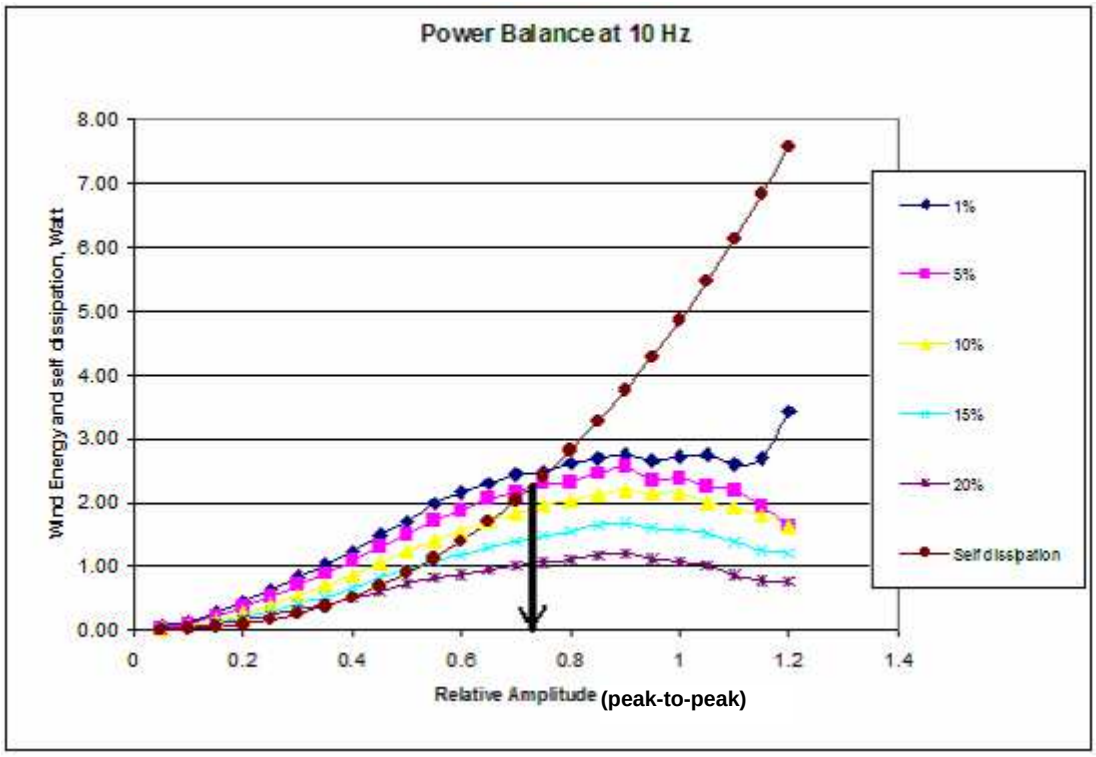

Figure 4.1 Power balance. The vibration amplitude is obtained at the crossing of the self dissipation curve with the wind power input curve. The arrow is giving the "balanced" amplitude for 5% turbulence wind input and self dissipation curve as given (for a defined frequency).

4 Endurance limit

The endurance limit of power lines conductors is related to broken strands. The next table is reproducing observed broken strands on conductors, including not only the outside layer but also inner layers.

Broken Outer Strands	Broken Inner-Layer Strands											
	0	1	2	3	4	5	6	7	8	9	10	11	12
0	117												
1	55	1		1									
2	66	4											
3	53	19	3				1						
4	16	21	13	3									
5	14	8	14	6	2								
6	10	8	17	12	3			1					
7	7	6	15	14	3								
8	7	5	6	7	7	3	1						
9	4	1	4	8	5	1							
10		1	4	1		1	1						
11	3			1	1	1							
12	2		1		1	1				1			
13			2										
14			1	1	1	1							
15		1		1									
16													
17													
18													

*All strand breaks were found at support clamps after line had been in service for approximately 25 years.

Table 5.1 Relative occurence of broken strands in inner and outer layers of ACSR cabel conductor 397.5 kcmil (30/7) (EPRI-1979)

Once the balanced amplitude is known at different frequencies, these data have to be analysed in terms of endurance limit. In fact these amplitudes are inducing alternate bending stress in conductors in each wave (the stronger stress at the larger radius of curvature) but of course any fixed point (like suspension clamps) will generate larger bending stress. Alternate bending stress will induce fatigue and are at the origin of many conductor problems in the field. (Electra-1985 b)

The endurance limit of conductors have been studied for many years and still subject of numerous investigations. Over 100 millions of cycles have to be tested which is time consuming and need appropriate test bench. The test has to reproduce appropriate actual conductor vibrations in its actual fittings and conditions (deflexion angle, presence of armor rods, flexibility of suspension clamp, ..) which is extremely difficult to manage (Electra- 1985 b)
Actual situation mix vibrations amplitudes of different frequencies, so that a method has to be found to combine these amplitudes/frequencies into one evaluation ("Miner"'s rules are geerally used but the approach is still controversial) (an example is treated in (Kiessling et al -2003, p 340)
During the fatigue test, conductor strands breaks have to be detected (which is not easy as they could occur in inner layers-generally the second one) and up to three strands break may be accepted.

The fatigue mechanism

The fatigue in power line conductors are caused by fretting between different layers of strands at their contact area (fig 5.1). Some cracks appear and propagate. The stick/slip elliptical contact area is depending on the radius of curvature taken by the conductor. During alternating bending stress (due to oscillations) that radius of curvature is changing continuously. It is particularly important near clamp ends at the last point of contact.

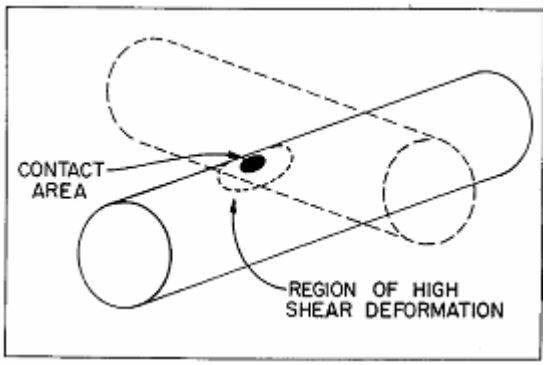

Fig 5.1 : the inter-strand contact area where first crack may appear (Epri-1979)

The amplitude of change of the radius of curvature is related to conductor data, particularly its bending stiffness and of course is depending on vibration amplitude and frequency (this last influencing the wave length, thus the slope near the clamp).

As mathematical modelling of a conductor is extremely difficult due to strands interactions, as bending stresses in the strands are difficult to measure, particularly in inner layers, these fatigue tests are done by measuring two quantities :

- either the bending amplitude Y_b , which is the amplitude of vibration measured at 89 mm from the last point of contact with the clamp (fig 5.2).

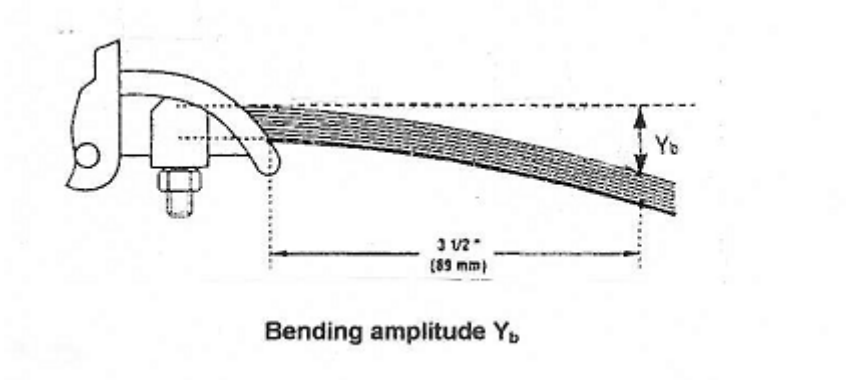

Fig 5.2 definition of bending amplitude.

- either (or simultaneously with the former one) the amplitude of vibration (more exactly the product f. y_{max} where f is the frequency of the vibration)

Difficulties are linked to :

- the y_{max} is difficult to measure in lab as it needs long span test (a minimum of several waves are needed), y_{max} may be strongly influenced in first waves by armor rod for ex.
- Y_b is difficult to be defined in some configurations (AGS, helical fixation, etc)

Endurance limit are defined in the litterature by at least one of these two basic data (Y_b or $f.y_{max}$). Sometimes but not always, lab tests have measured both these values during the same test which is very helpful.

The litterature tranfer these two data measured during fatigue test or measure in actual situation, into bending strain (which may easily be converted into microstrain) by a mathematical model. The PS (Poffemberger-Swart – 1965) formula is then used but many discussion exist about that.

$$\varepsilon = \frac{Y_b d}{2j^2\left(e^{-A/j} - 1 + \frac{A}{j}\right)} \qquad \text{(eq 5.1)}$$

where

ε = microstrain (microinches/inch or microcm/cm)

Y_b = bending amplitude

d = diameter of outside lay *strand*

A = length of measuring arm (3.5 inches or 89 mm)

$j = \sqrt{EI_{min} / H}$

H= conductor tension

I_{min} = minimum moment of inertia of cross-section of *total* conductor

E = Young's modulus for the *total* conductor

Strain, being a dimensionless unit, is the same figure in English or S.I. units. The term *A/j* is also dimensionless. Since the tabulated values of EI_{min} are given in 1bf•in^2 and Nm^2 it is convenient in solving the problems in S.I. units to express lengths in meters and force in Newtons. Solving for Drake conductor at 20% Rated Strength and 10 mils (=0.254mm) bending amplitude:

	English	*S.I.*
EI =	15,469 lb in^2	44.39 N•m2
H =	6,300 lb	28,024 N
Y_a =	0.01 in	2.54 x 10^{-4}m
d =	0.1749 in	4.44 x 10^{-3}m
A =	3.5 in	8.89 x 10^{-2}m
A/j =	2.234	2.234

Solving Equation (eq 5.1) for the above values:

ε =	266 x 10^{-6}	266 x 10^{-6}

There is also another expression to convert vibration amplitude (0 to peak) into bending strain :

$$\sigma_a = \pi d E_a \sqrt{\frac{m}{EI}} f y_{\max} \qquad (eq \quad 5.2)$$

where σ_a is the stress in outer layer, d is diameter of outer layer strand, f is the frequency (Hz), y_{max} is the antinodal displacement (**half** of pk-pk amplitude), E_a is the modulus of elasticity of last layer material (generally, Aluminium (68950 Mpa)), m is the conductor mass per unit length and EI the (whole) conductor bending stiffness.

Two extreme possibilities exist for the bending stiffness, EI_{min} & EI_{max}. The difference between these two extremes can be as much as 70 times. The "Orange Book" would indicate that for problems, which relate to conductor strain in the outer layer, a figure approaching EI_{min} would apply.

It needs the strands detail of conductor to calculate the value of EI_{min}. This calculation is explained in many places as (EPRI-1979 or more recently "Overhead power lines" – 2003)

Once the bending stress is known, it can be converted into strain by Hooke relationship, generally the strain is expressed in microstrain.

ENDURANCE LIMITS
FOR VARIOUS TYPES OF CONDUCTORS*
SI Units

Conductor Type	σ_a / fy_{max}	*Endurance Limit* σ_a	fy_{max}
All-Aluminum	0.172 MPa-sec/mm	22 MPa	128 mm/sex
All-5005 Alloy	0.172	22	128
All-Aldrey or 6201	0.172	15	87
ACSR (Except 7 / 1)	0.186	22	118
ACSR (7 / 1)	0.148	22	149
Copper (Cu)	0.409	35	86
Copperweld (Cw)	0.299	35	117
6 Cu/1 Cw	0.377	35	93
2 Cu/1 Cw	0.359	35	97
EHS Steel (Galv.)	0.499	192	385
(Aluminized)	0.497	135	272
Alumoweld	0.498	135	276

Table 5.2 : fatigue performance relative to bending amplitude (source EPRI-1979)

Maximum Safe Bending Amplitudes For ACSR

Name	Conductor Size (kcmils)	Stranding	Tension in Percent of Rated Strength* 15% y_b		25% y_b		35% y_b	
			mm	mils	mm	mils	mm	mils
Turkey	# 6	6 / 1	0.97	38.	0.79	31.	0.69	27.
Swan	4	6 / 1	0.92	36.	0.76	30.	0.67	26.
Swanate	4	7 / 1	1.01	40.	0.84	33.	0.74	29.

Sparrow	2	6 / 1	0.86	34.	0.73	29.	0.64	25.
Sparate	# 2	7 / 1	0.94	37.	0.80	31.	0.71	28.
Robin	# 1	6 / 1	0.82	32.	0.70	28.	0.63	25.
Raven	# 1/0	6 / 1	0.79	31.	0.68	27.	0.61	24.
Quail	2/0	6 / 1	0.75	30.	0.66	26.	0.59	23.
Pigeon	3/0	6 / 1	0.71	28.	0.63	25.	0.57	22.
Penguin	# 4/0	6 / 1	0.67	26.	0.59	23.	0.54	21.
Waxwing	266.8	1 8 / 1	0.33	13.	0.28	11.	0.26	10.
Owl	266.8	6 / 7	0.22	9.	0.20	8.	0.18	7.
Partridge	266.8	26 / 7	0.32	12.	0.26	10.	0.23	9.
Merlin	336.4	1 8 / 1	0.31	12.	0.27	11.	0.24	10.
Linnet	336.4	26 / 7	0.30	12.	0.26	10.	0.23	9.
Oriole	336.4	30 / 7	0.32	13.	0.27	11.	0.24	9.
Chickadee	397.5	1 8 / 1	0.30	12.	0.26	10.	0.24	9.
Brant	397.5	24 / 7	0.29	11.	0.25	10.	0.22	9.
Ibis	397.5	26 / 7	0.30	12.	0.25	10.	0.22	9.
Lark	397.5	30 / 7	0.31	12.	0.26	10.	0.23	9.
Pelican	477.O	1 8 / 1	0.29	11.	0.25	10.	0.23	9.
Flicker	477.0	24 / 7	0.28	11.	0.24	10.	0.22	9.
Hawk	477.0	26 / 7	0.28	11.	0.24	10.	0.22	9.
Hen	477.0	30 / 7	0.30	12.	0.26	10.	0.23	9.
Osprey	556.5	1 8 / 1	0.27	11.	0.24	10.	0.22	9.
Parakeet	556.5	24 / 7	0.27	11.	0.24	9.	0.21	8.
Dove	556.5	26 / 7	0.28	11.	0.24	9.	0.21	8.
Eagle	556.5	30 / 7	0.29	11.	0.25	10.	0.22	9.
Peacock	605.0	24 / 7	0.27	10.	0.23	9.	0.21	8.
Squab	605.0	26 / 7	0.27	11.	0.23	9.	0.21	8.
Teal	605.0	30 / 19	0.26	10.	0.22	9	0.20	8.
Swift	636.0	36 / 1	0.32	13.	0.28	11.	0.26	10.
Kingbird	636.0	18/ 1	0.26	10.	0.24	9.	0.22	9.
Rook	636.0	24 / 7	0.26	10.	0.23	9.	0.21	8.
Grosbeak	636.0	26 / 7	0.27	11.	0.23	9.	0.21	8.
Egret	636 .O	30/ 19	0.26	10.	0.22	9.	0.20	8.
-	653.9	1 8 / 3	0.26	10	0.23	9.	0.21	8.
Flamingo	666.6	24 / 7	0.26	10.	0.23	9.	0.21	8.
Gannet	666.6	26 / 7	0.26	10.	0.23	9.	0.21	8.
Starling	71 5.5	26 / 7	0.26	10.	0.23	9.	0.21	8.
Redwing	71 5.5	30/ 19	0.25	10.	0.22	9	0.20	8.
Coot	795.0	36 / 1	0.31	12.	0.27	11.	0.25	10.
Tern	795.0	45 / 7	0.30	12.	0.26	10.	0.24	9.
Cuckoo	795.0	24 / 7	0.25	10.	0.22	9.	0.20	8.
Condor	795.0	54 / 7	0.32	12.	0.27	11.	0.24	10.

*For other tensions, interpolate between values given.

Name	Conductor Size (kcmils)	Stranding	15% y_b		25% y_b		35% y_b	
			mm	mils	mm	mils	mm	mils
Drake	795.0	26 / 7	0.25	10.	0.22	9.	0.20	8
Mallard	795.0	30 / 19	0.25	10.	0.21	8.	0.19	8
Ruddy	900.0	45 / 7	0.30	12.	0.26	10.	0.23	9
Canary	900.0	54 / 7	0.31	12.	0.27	10.	0.24	9
Catbird	954.0	36 / 1	0.29	11.	0.26	10.	0.24	9
Rail	954.0	45 / 7	0.29	12.	0.26	10.	0.23	9
Cardinal	954.0	54 / 7	0.30	12.	0.26	10.	0.24	9
Ortolan	1033.5	45 / 7	0.29	11.	0.25	10.	0.23	9
Curlew	1033.5	54 / 7	0.30	12.	0.26	10.	0.23	9
Bluejay	1113.0	45 / 7	0.28	11.	0.25	10.	0.22	9
Finch	1113.0	54 / 19	0.28	11.	0.24	9.	0.22	9
Bunting	1192.0	45 / 7	0.28	11.	0.24	10.	0.22	9

Grackle	1192.0	54 / 19	0.27	11.	0.24	9.	0.21	8
Bittern	1272.0	45 / 7	0.27	11.	0.24	9.	0.22	9
Pheasant	1272.0	54 / 19	0.27	11.	0.24	9.	0.21	8
Dipper	1351.5	45 / 7	0.27	11.	0.24	9.	0.22	9
Martin	1351.0	54 / 19	0.27	11.	0.23	9.	0.21	8
Bobolink	1431.0	45 / 7	0.26	10.	0.23	9.	0.21	8
Plover	1431.0	54 / 19	0.26	10.	0.23	9.	0.21	8
Nuthatch	1510.5	45 / 7	0.26	10.	0.23	9.	0.21	8
Parrot	1510.5	54 / 19	0.26	10.	0.23	9.	0.21	8
Lapwing	1590.0	45 / 7	0.26	10.	0.23	9.	0.21	8
Falcon	1590.0	54 / 19	0.26	10.	0.23	9.	0.20	8
Chukar	1780.0	84 / 19	0.29	11.	0.25	10.	0.23	9
—	2034.0	72 / 7	0.28	11.	0.25	10.	0.23	9
Bluebird	2156.0	84 / 19	0.28	11.	0.24	10.	0.22	9
Kiwi	2167.0	72 / 7	0.27	11.	0.24	10.	0.22	9
Thrasher	2312.0	76 / 19	0.27	11.	0.24	9.	0.22	9
Joree	2515.0	76 / 19	0.26	10.	0.23	9.	0.21	8

*For other tensions, interpolate between values given.

Table 5.3 : fatigue performance relative to bending amplitude (source EPRI-1979), for different sagging conditions.

Estimated Bending Amplitude Endurance Limits For Various Types Of Conductor

Conductor	Tension	Y_b Endurance Limit	
		mm	mils
7 No. 8 Alumoweld	25%	0.96	38
7 No. 6Alumoweld	25%	0.96	38
123.3 kcmil 5005 (7 str)	25%	0.59	23
123.3 kcmil 6201 (7str)	25%	0.40	16
¾" EHS Steel (7 str)	25%	1.96	77
½" EHS Steel (7 str)	25%	1.67	66

Table 5.4 : fatigue performance relative to bending amplitude (source EPRI-1979)

The endurance limit is generally considered when maximum three broken strands are observed.

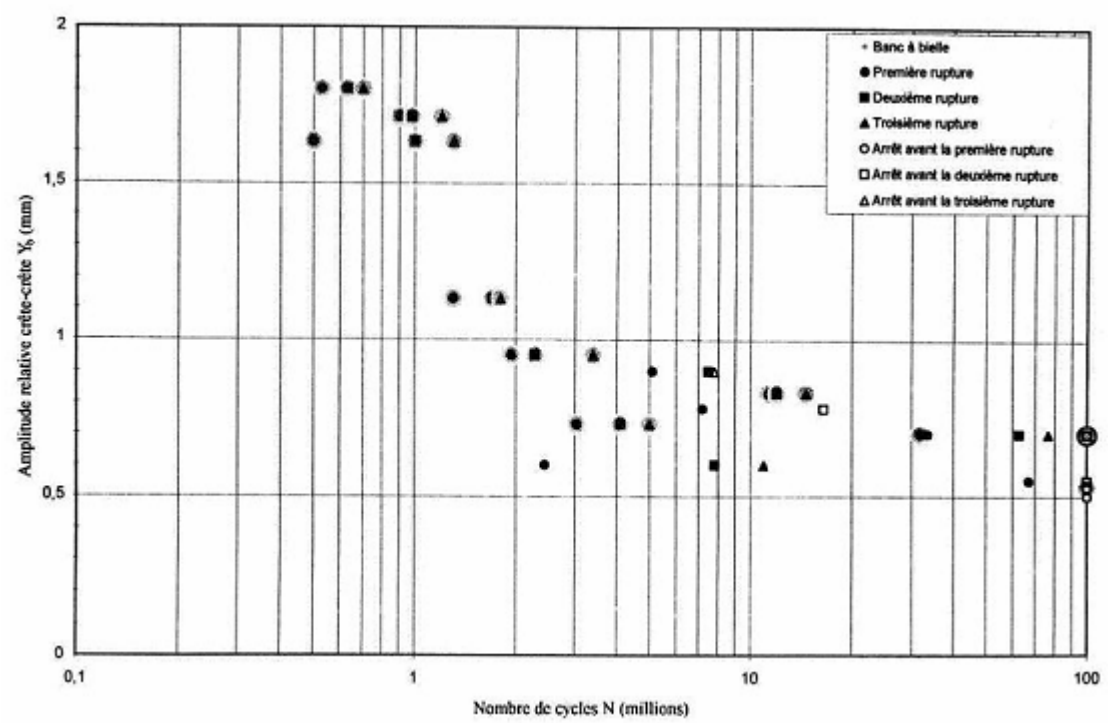

Fig 5.3 typical fatigue diagram obtained on test bench (courtesy L. Cloutier, Sherbrooke). Essai sur banc à bielle, pince rigide. OPGW 22.9 mm diameter (fiber optic tube 6.5 mm, 8 alumoweld strands layer followed by 14 aluminium-alloy strands (4.1 mm), 20%RTS = 0.20 x 171 kN = 34.2 kN) (frequencies between 38 and 44 Hz)

Numerous investigation of actual line vibrations measurement is detailed in the litterature (Diana-1982, Hardy-1991, Electra-1995)

5 Earthwires and OPGW

Earthwire and OPGW have generally lower external diameter compared to phase conductor, this is inducing, due to Strouhal relationship (eq 3.1), at typical wind speed for Von Karman vortex shedding, vibration frequencies at higher level (up to 150 Hz and even over have been observed) with amplitude up to 300 mils (=7,5 mm) (Rawlins, 1986) at 16 inches (40,6 cm) (from support).
OPGW, due to their constitution, with less layers, thus less contact zone between strands have lower self damping and even it has been measured that there could be very sensible decrease of self damping with age of the conductor (by a factor 8 in 20 years following Rawlins-1986).
Earthwire and OPGW due to their lower diameter and absence of current flow and their top altitude position on tower may aggregate more ice/snow during such event. In presence of ice/snow the apparent diameter being much larger may generate aeolian vibrations of higher amplitudes (maximum amplitude is related to diameter for fluid reasons) with larger damages.

5.1 OPGW clamping systems

OPGW end clamp are very different from phase conductor. A recent enquiries evaluated the proportion of use of each of these clamps (fig 6.1 to 6.5).

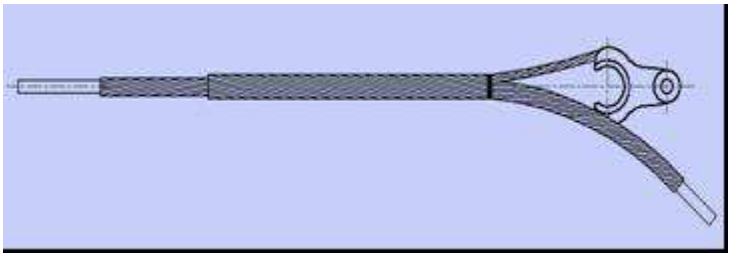

Fig 6.1 So called “helical” dead-end clamp (more than 40 % in CIGRE enquiry)

Aluminium covered stell (alumoweld) is used for the wires of the preform, the number and diameter of the wires are designed for mechanical strength purposes and for compatibility with the aluminium alloy and alumoweld wires of the OPGW. The vibration fatigue limit of the preform is not calculated but preforms are tested on the OPGW, typically 100 Mcycles at resonant frequency (Smart-1999). Grade of alumoweld (typical 10% nominal wire radius thickness) is generally the same for OPGW and the preform. The OPGW should exit the preformed deadend in a smooth arc with a radius greater than the minimum bend radius given by the manufacturer of the OPGW. This is function of the overall diameter of the OPGW and is normally 20 times the diameter. The OPGW should not be “kinked” or deformed in this area. Generally preformed deadend has a set of armour rods installed on the OPGW with the preform over these armour rods. The armour rods and the preform should be oppossite lay (RH onto LH) to cancel out the torsion.

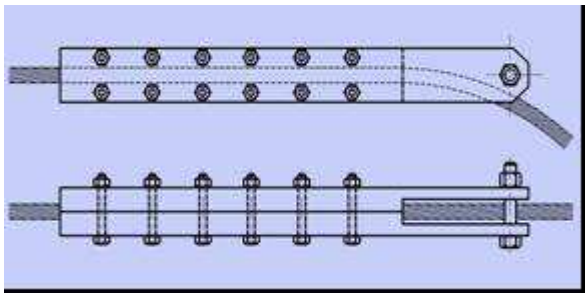

fig 6.2 so called “bolted” dead-end clamp (more than 10% in CIGRE enquiry)

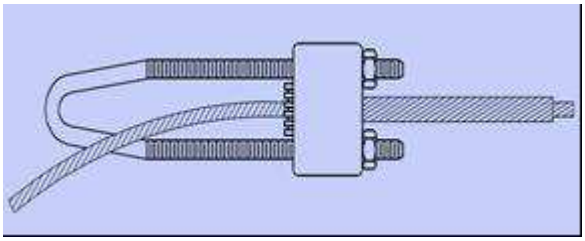

fig 6.3 so called “conical” dead-end clamp (more than 15% in CIGRE enquiry)

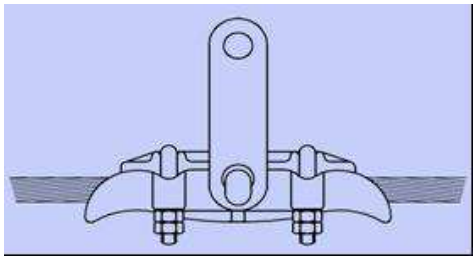

fig 6.4 so called “bolted” clamp (suspension) (more than 15% in CIGRE enquiry)

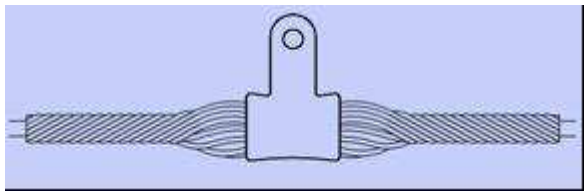

fig 6.5 so called “Armor Grip” suspension clamp (more than 50% in CIGRE enquiry)

5.2 Test Procedures - Fittings for OPGW on overhead lines

Test Procedures - Fittings for OPGW on overhead lines

TENSION FITTING

- Cyclic tensile load*
- Aeolian vibration fatigue*
- Galloping fatigue*
- Fault current

SUSPENSION FITTING

- Vertical load/turning angle*
- Aeolian vibration fatigue*
- Galloping fatigue*
- Fault current
- Unbalanced load to IEC 61284

* Increase in optical attenuation when loaded upto SMWT < 0.05 dB/km at 1550 nm

CIGRE Tutorial PB POWER

Test Procedures - Fittings for OPGW on overhead lines

VIBRATION DAMPER

- Application test*
- Reference to IEC 61897 for Stockbridge dampers
- Anti-node velocity < 500 mm/sec for Impact dampers

ANTI-GALLOPING DEVICE

- Application test*
- Required to limit galloping

AIRCRAFT WARNING DEVICE

- Application test*

GROUND CONNECTORS

- Application test*

DOWNLEAD CLAMP

- Application test*

* Increase in optical attenuation when loaded upto SMWT < 0.05 dB/km at 1550 nm

CIGRE Tutorial PB POWER

There exist a large litterature on the subject, f.e. (Electra-1994 & 1996 & 1998, Smart-1999, IEEE-1994, Bellcore standard-1994).
Guide to Test Procedures of Fittings for OPGW & OPPC was published in Electra No 188, February 2000

6 Analysis of Safe Design Tension

Guidance to the safe design tension with respect to Aeolian vibration has been worked out by CIGRE (Electra- 1999) by the so-called EDS panel. The experienced showed that the safe design tension in terms of percentage of RTS (Rated Tensile Strength) is insufficient to explain the fatigue damage. Therefore it is now considered to use the ratio H/W between the horizontal tensile load and the weight per unit length of conductor rather than % of RTS. It mainly is that the use of percentage of the conductor breaking strength is misleading as the conductor breaking strength has no direct relation to its damping properties nor to its endurance capability. The catenary parameter H/w is an image of mean conductor radius of curvature, it mixes both stress in the conductor (tension/cross section) and conductor volumic mass.

The rating parameter, $Ld/\sqrt{Hm}$, (where L is actual span length, d is conductor diameter, H is horizontal tension in the conductor and m is mass of the conductor per unit length) has been used in analysis of collection of field experience data on fatigue overhead conductors to rank spans according to the difficulty in damping them, based on the line design variables, span length, conductor size and tension.

The parameter is proportional to the damping efficiency required to control vibration amplitude to a given level. Since the CIGRE had adopted the parameters H/W, to rate the effect of tension on conductor self- damping, it was able to simplify the set of rating parameters $Ld/\sqrt{Hm}$ to Ld/m and H/W (Electra- 1999 & 2005 a). Fig 7.1 is giving the CIGRE curve for terrain category 1 and fig 7.2 is showing about 20 existing cases with and without problems. The four belgian cases under investigation have been inserted.

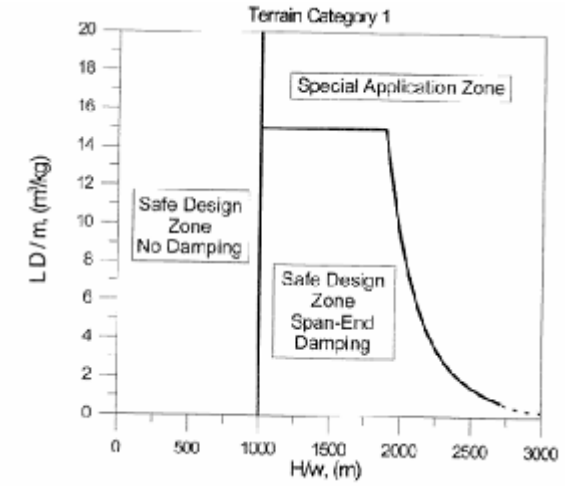

Figure 7.1 Recommended safe design tension for single conductor lines. H: initial horizontal tension (N); w: conductor weight per unit length (N/m); D: conductor diameter (m); m: conductor mass per unit length (kg/m). Terrain no. 1: open, flat, no trees, no obstruction, with snow cover, or near/across large bodies of water; flat desert. Data on other terrains are available in [Electra -1999 & 2005 a].

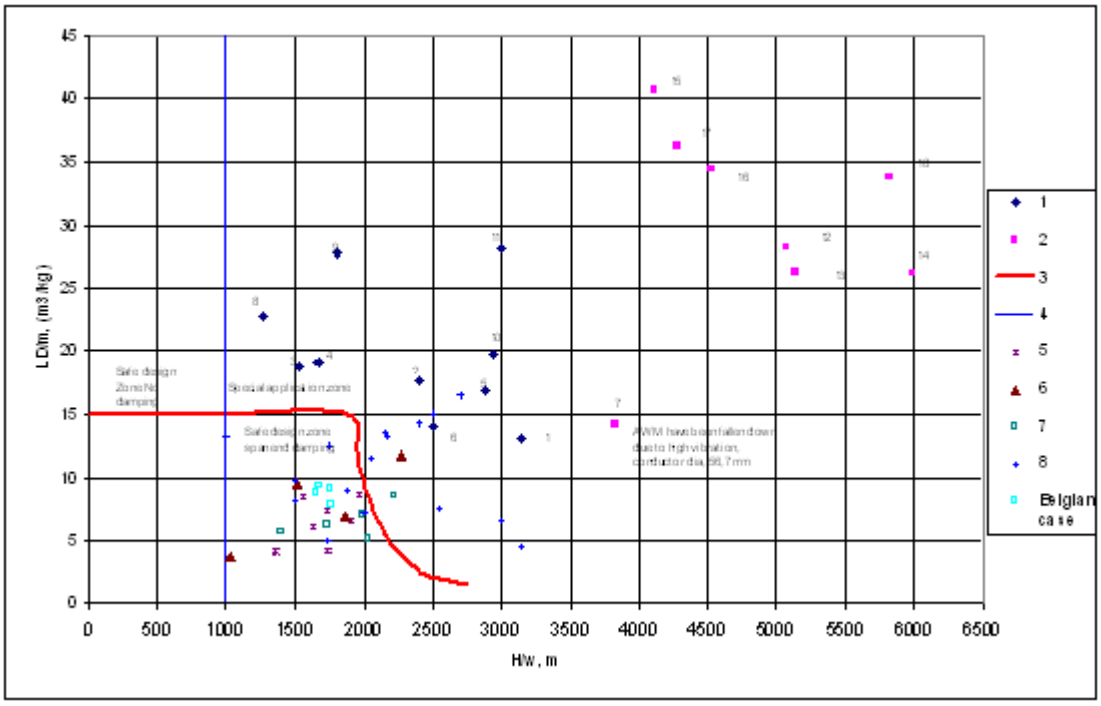

Figure 7.2 : CIGRE Safe boundaries according to endurance limit approach. Basic dots are coming from known cases with/without problems. The four cases of belgian cases have been added.

Based on this diagram, it is apparent that the four belgian cases would need dampers.

7 Stockbridge-type damper

The power dissipated by damper may be evaluated on basis of complex impedance characteristic defined as follows.(Leblond-1999)

By supposing the velocity of the system varying by harmonic law,

$$\dot{y}(t) = \dot{y}_0 \sin \omega t \,, \qquad \text{(eq 7.1)}$$

the corresponding force upon the damper reads

$$F(t) = Z_{11} \dot{y}_0 \sin\left(\omega t + \alpha_{11}\right). \qquad \text{(eq 7.2)}$$

Here, the coefficients Z_{11}, α_{11} can be determined experimentally as functions of ω and possibly also of the velocity amplitude $\dot{y}_0$. Complex impedance coefficient then reads $z_{11} = Z_{11} e^{i\,\alpha_{11}}$ or $z_{11} = R_{11} + iI_{11}$ where

$$R_{11} = Z_{11} \cos \alpha_{11},\ I_{11} = Z_{11} \sin \alpha_{11}\,. \qquad \text{(eq 7.3)}$$

The plots of characteristic impedance curves for a measured damper is shown in the figures below.

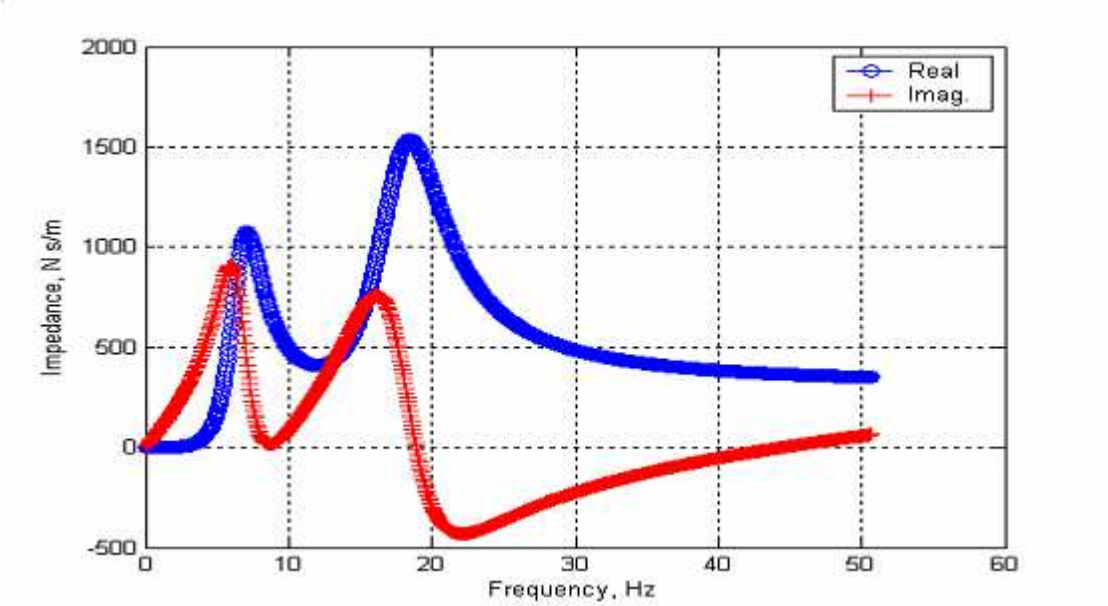

Fig 8.1 Impedance curves of typical stockbridge type damper
(taken at the speed of 100 mm/s). Real and Imag of Z_{11}.

The evaluation of how many dampers and where to install them is basically evaluated by energy balanced method using their energy response generally obtained on shaker tests.

But the experience has pointed our these facts (Electra-2005 b) :

- the behaviour of dampers is non linear , their response is depending on the excitation. Generaly damper impedance is evalutated for clamp velocity speed up to 100 mm/s
- the damper is not reacting only on vertical, it means that vibrations would induce vertical force reaction at the damper location but also a rocking moment. Both influence the conductor shape near the clamp. So that damper-conductor is a system which would have to be analysed all together. Actual recommendation is to perform test on 60 m span length in lab using conductor + damper system to evaluate efficiencies. This is extremely costly and time consuming but probably the best way to evaluate properly the interactions.
- The location of damper is basically oriented on the fact that a damper at anti-node position would have the best efficiency (as the amplitude will be the largest, and so for the speed). But , as a range of wind speed has to be considered, a range of frequencies has to be looked at. So that damper is never located at its optimal position for one case.

Some of these aspects are discussed in recent papers (Electra- 2005 b). Procedure for damper tests are explained in (IEEE-1993 and IEC 61897)

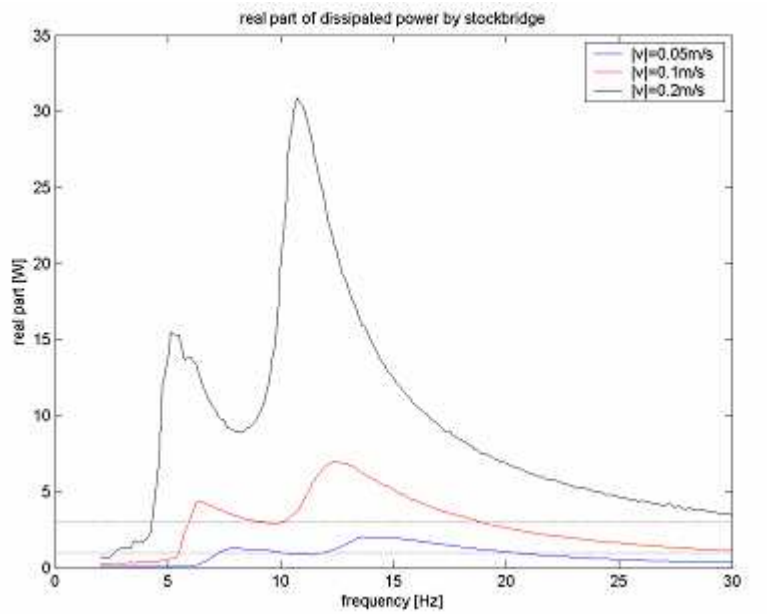

Fig 9.2 power dissipation (in Watts) obtained by a Stockbridge of 12.5 kg, as measured in our lab. Horizontal dotted lines given for 1 and 3 Watts dissipation.

8 Conclusions

Aeolian vibration is an important sollicitation of power lines and earthwires. It may be the cause of conductor alternate bending stress near clamp ends which may suffer millions of cycles per year. The endurance limit of power lines cables, OPGW and other cable have been tested in some lab.

The physics of fretting fatigue is extremely complex and the fatigue phenomenon is influenced by the clamping system.

OPGW – earthwires.

The major concern is for the OPGW and earthwires that are the cause of numerous aeolian vibrations as their position on the tower and their diameter (lower than phase conductor) are generating more opportunities of numerous vibration cycles.

OPGW are even worst as they have limited layers of wires, thus limiting self damping. Thus OPGW may suffer large amplitude vibrations at relatively high frequencies.

But material of earthwires and OPGW are generally made of alumoweld, having much higher endurance limit compared to AAAC.

Clamping system is a key point. A case by case analysis has to be perfomed but generally span length larger than 100 m in environment favouring aeolian vibrations (limited turbulence) have to be protected if their catenary parameter is larger than 1000 meters (open, flat, no trees, no obstructions) up to 1425 meters (built-up with some trees and buildings, small towns,..).

Phase wires

Phase wires may also suffer major trouble and their material of the outside layer (aluminium) has a very limited endurance limit. Cases in flat terrain need appropriate protection.

9 References

1. J.C Poffemberger, R.L. Swart. 1965. *Differential displacement and dynamic conductor strain*. IEEE Trans. PAS-84, 1965, pp 281-289, Discussion pp. 508-513, Errata p.732
2. W.F. Buckner, H. Kerner, W. Philipps. 1968. *Stresses in Transmission Line Conductors Near the Suspension Clamp.* Cigre plenary session, Report 22-07.
3. R. Claren, G. Diana 1969. *Mathematical Analysis of Transmission Line Vibration*. IEEE Trans. On PAS-88 No 12
4. R. Claren, G. Diana, Nicolini 1974. *Vibration in Multiple Conductor Bundles*. CIGRE plenary session, report 22-8.
5. EPRI- 1979. *Transmission Line Reference Book: Wind-Induced Conductor Motion*, Electric Power Research Institute, Palo Alto, CA.
6. Electra- 1979 a. *Guide on conductor self-damping measurements*. N° 62. (identical to IEEE 563-1978 Standard)
7. Electra- 1979 b. *Recommendation for evaluation of lifetime of transmission line conductors.* Electra N°63.
8. G. Diana, Gasparetto, F. Tavano, U. Cosmai. 1982. *Field measurement and field data processing on conductor vibration (Comparison between experimental and analytical results).* CIGRE plenary session, 1982.
9. P. Hagedorn, 1982. *On the computation of damped wind-excited vibrations of overhead transmission lines*, *Journal of Sound and Vibration,* 83(2), 253-271.
10. Electra – 1985. report '*Guide for endurance testing of conductor inside clamp'*, ELECTRA N°100, page 77-86.
11. C. Rawlins 1986 *Research on vibration of overhead ground wires*. IEEE Trans on Power Delivery, presented at IEEE/PES 1986 meeting in Anaheim, California.
12. Electra-1988. *Modelling of Aeolian Vibration of Single Conductors: Assessment of the Tecnology.* Electra No. 181.
13. R.D. Blevins, "Flow Induced Vibration", Van Nostrand Reinhold, New York, Second Edition 1990.
14. C. Hardy, J. Brunelle 1991. *Principles of measurement and analysis with the new Pavica conductor vibration recorder.* CEA report (Canadian Electrical Association).
15. IEEE – 1993. *Guide for laboratory measurement of the power dissipation characteristics of aeolian vibration dampers for single conductor*. IEEE Standard 664-1993
16. Electra-1994. CIGRE technical brochure '*Optical Fibre Planning Guide for Power Utilities*', ELECTRA N° 157.
17. Bellcore Standard '*Generic requirements for Fibre Optic Splice Closures'* GR-771-CORE, Issue 1, July 1994.
18. Electra 1995*. Guide to vibration measurements on overhead lines*. Electra n. 163.
19. Electra 1996. CIGRE report '*Results of the Questionnaire-Fittings for Fibre Optic Cables on Overhead Lines'*, ELECTRA N°165.
20. C.B. Rawlins 1998. *Model of power imparted to a vibrating conductor by turbulent wind*, Technical note no. 31, ALCOA Conductor Products Company, November 1998.
21. Electra 1998. CIGRE report '*Guide to Fittings for Optical Cables on Transmission Lines, Part 1 – Selection and Use'*, ELECTRA N° 176.
22. Electra 1998. *Modelling of aeolian vibrations of single conductors-assessment of technology*. Electra N° 181.
23. IEC Standard 61897 '*Requirements and tests for stockbridge type aeolian vibration dampers*'. 1998

24. Electra 1999. "*Safe design tension with respect to aeolian vibrations, part 1: single unprotected conductors*", Electra N° 186.
25. T. Smart et al 1999. *Guide to fittings for optical cables in Transmission Lines.* Document interne au CE 22, WG11, TF3. Also presented during a tutorial at the CIGRE session in Paris 2004 (SCB2)
26. A. Leblond, C. Hardy, 1999 « *On estimation of 2x2 complex stiffness matrix for symmetric Stockbridge type dampers* », *Proc. 3rd Symposium on Cable Dynamics,* Trondheim, 139-144.
27. Verma H., Chakraborty, G., Krispin, H-J., Hagedorn, P., 2003 *The modelling of wind induced vibrations of long span electrical overhead transmission lines*", *Proc. Vth Symp. On Cable Dynamics,* Santa Margherita Ligure, 53 – 60, 2003.
28. F. Kiessling, J.F. Nolasco, P. Nefzger, U. Kaintzyk. 2003 *Overhead power lines*. Springer-Verlag. ISBN 3-540-00297-9.
29. Electra 2005 a. "*Safe design tension with respect to aeolian vibrations, part 2: single damped conductors*", Electra N° 190.
30. Electra 2005 b. „*Modelling of aeolian vibrations of a single conductor plus damper : assessment of technology*", Electra N° 223 , pp 28-36.
31. IEEE 1138-1994 '*Standard construction of Composite Fibre Optic Overhead Ground Wire [OPGW] used on Electric Utility Power Lines'*.